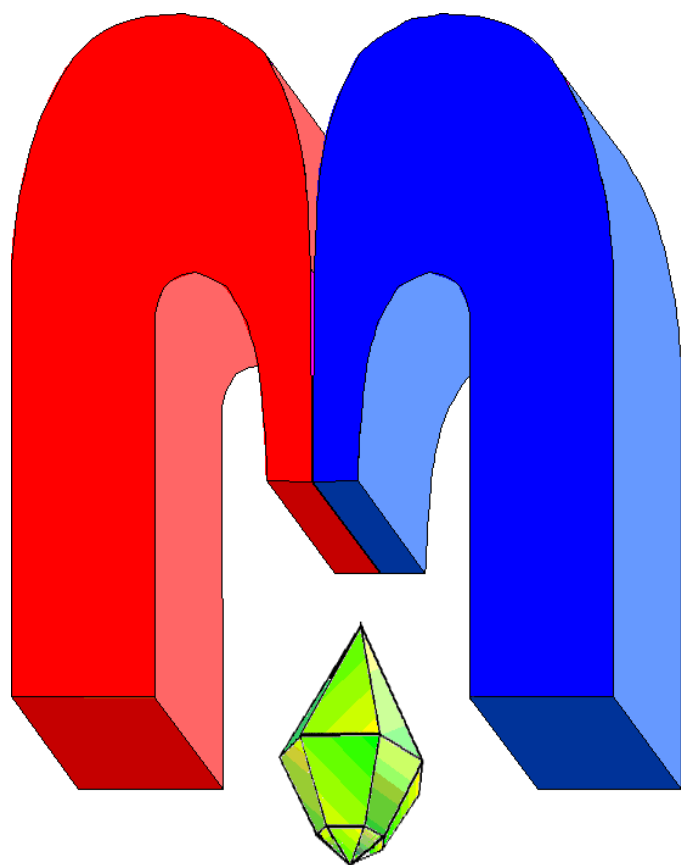


ISSN 2072-5981



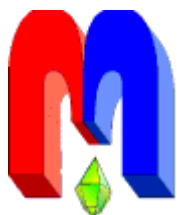
***Magnetic
Resonance
in Solids***

Electronic Journal

Volume 15, 2013

No. 1, 13103 – 11 pages

<http://mrsej.ksu.ru>



Established and published by Kazan University
Sponsored by International Society of Magnetic
Resonance (ISMAR)
Registered by Russian Federation Committee on Press,
August 2, 1996
First Issue was appeared at July 25, 1997

© Kazan Federal University (KFU)*

"*Magnetic Resonance in Solids. Electronic Journal*" (**MRSej**) is a peer-reviewed, all electronic journal, publishing articles which meet the highest standards of scientific quality in the field of basic research of a magnetic resonance in solids and related phenomena. **MRSej** is free for the authors (no page charges) as well as for the readers (no subscription fee). The language of **MRSej** is English. All exchanges of information will take place via Internet. Articles are submitted in electronic form and the refereeing process uses electronic mail. All accepted articles are immediately published by being made publicly available by Internet (<http://MRSej.ksu.ru>).

Editors-in-Chief

Jean **Jeener** (Universite Libre de
Bruxelles, Brussels)
Boris **Kochelaev** (KFU, Kazan)
Raymond **Orbach** (University of
California, Riverside)

Executive Editor

Yurii **Proshin** (KFU, Kazan)
Editor@ksu.ru

Editors

Vadim **Atsarkin** (Institute of Radio
Engineering and Electronics, Moscow)
Detlef **Brinkmann** (University of Zürich,
Zürich)
Yurij **Bunkov** (CNRS, Grenoble)
John **Drumheller** (Montana State
University, Bozeman)
Mikhail **Eremin** (KFU, Kazan)
David **Fushman** (University of Maryland,
College Park)
Yoshio **Kitaoka** (Osaka University, Osaka)
Boris **Malkin** (KFU, Kazan)
Haruhiko **Suzuki** (Kanazawa University,
Kanazava)
Murat **Tagirov** (KFU, Kazan)

*

In Kazan University the Electron Paramagnetic Resonance (EPR) was discovered by Zavoisky E.K. in 1944.

TEMPOL as a polarizing agent for dynamic nuclear polarization of aqueous solutions

M.R. Gafurov

Kazan Federal University, Institute of Physics, Kremlevskaya, 18, Kazan 420008, Russia

E-mail: Marat.Gafurov@kpfu.ru

(Received March 19, 2013; accepted April 9, 2013)

High-resolution proton NMR (400 MHz) and multifrequency EPR (9 – 260 GHz) characterization of aqueous solutions of the nitroxyl radical TEMPOL in the temperature range (10 – 40) °C is performed for the liquid-state DNP. Characteristic features of the in-situ DNP observations at high frequencies are presented. Optimal conditions (concentration, temperature, position of the microwave pumping, repetition/build-up time for the DNP experiments) are extracted. The results are compared with the DNP experiments, molecular dynamic calculations, saturation models, and classical models of translational and rotational diffusion. Perspectives for using TEMPOL as polarizing agent in even higher magnetic fields are discussed.

PACS: 76.30.-v, 76.60.-k, 76.70.Fz

Keywords: DNP, NMR, EPR, Overhauser effect, polarizing agent, nitroxide

1. Introduction

The possibility to increase nuclear magnetic resonance (NMR) signal-to-noise ratio significantly by spin polarization transfer from the electronic spin S to the coupled nuclear one of interest I attracts last decade heightened attention regarding applications in magnetic resonance imaging (MRI), structural biology, analytical chemistry, NMR petrophysics, material science, investigations of nano- and micro samples and flows in low and high magnetic fields, etc [1-3]. Nowadays it is achieved by different methods and techniques determined mainly by a variety of physical mechanisms of dynamic nuclear polarization (DNP) such as the cross effect, thermal mixing, the solid effect and the Overhauser effect (OE). While the first three are efficient in solid state, the OE DNP is the most effective in liquids and shows up even in systems wherein microwave (MW) polarization of S and NMR detection take place in the same magnetic field at the same temperature.

A proper choice of polarizing agents for each of the DNP techniques used play a key role for the DNP yield. Understanding the background underlying the processes leads to the synthesis of new, more effective materials and exploiting them under optimal conditions. A list of “older” radicals used for DNP and their characterization were compiled in [4], for example. The most commonly used polarizers now are trityl (triarylmethyl), nitroxide (nitroxyl) radicals, their combinations and derivatives [1-3].

This work presents a systematic NMR and EPR (electron paramagnetic resonance) experimental studies of aqueous solutions of the stable nitroxide TEMPOL and their comparison with the high-field DNP results under continuous wave irradiation at near room temperatures of (10-40) °C as well as with the previously developed models and calculations.

2. Theoretical background and literature review

This section contains the information which is essential for the understanding of OE DNP mechanisms along with the relevant review of the known for author experimental and theoretical research in this direction conducted last years.

For a long time in-situ liquid state (LS) polarization experiments, in which MW polarization and NMR detection take place in the same magnetic field at the same temperature, were not considered as a valuable option in high magnetic fields (HF) due to the hardware and theoretical problems. Firstly, until recently high-power MW sources for high MW frequencies to saturate EPR transitions were not commercially available on the market and they are still expensive as well as transmission lines. Secondly, high dielectric losses of water needed for the most biological and oil research applications cause an extensive microwave heating of aqueous samples even at low MW power levels demanding tremendous efforts in the construction of the hardware setup. Thirdly, the theory based on the DNP experiments carried out in 1950s-1970s in the magnetic fields less than 1.5 T [3-6] predicted a miserable DNP enhancement for higher magnetic fields for liquids in which Overhauser effect plays a primary role [7, 8]. Last year experiments [1-3] reveal not only perceptible but significant OE DNP enhancements for protons of liquids in the fields of (3.4-9.2) T showing that the long established models cannot adequately describe new results and, therefore, additional experimental and theoretical research in such high fields should be done.

To flip nuclear spin I , the energy of its interaction with S should be time-dependent, i.e. fluctuating local magnetic field, B_{local} , should exist Fourier component of which with ω_I would cause nuclear spin reorientation. DNP experiments in low magnetic fields were and still are explained using translational motion (diffusion) of the molecules in the solvent with τ_{tr} in which the characteristic time, τ , for the isotropic diffusion is given as

$$\tau \approx \tau_{\text{tr}} = \frac{d^2}{D_W + D_R}, \quad (1)$$

where d is a distance of the closest approach between S and I , D_W and D_R are the diffusion coefficients of diamagnetic particles (water or molecules of other solvent) and paramagnetic radical, correspondingly. Electronic spin-lattice (longitudinal) and spin-spin (transverse) relaxation with T_{1e} and T_{2e} for aqueous solutions of nitroxides are much longer and are not considered as sources of nuclear re-orientation in OE DNP driven mechanism.

The results of Ref. [9] focused on comparison of the nitroxide TEMPO-based mono- and bi-radicals prove that even in high fields (9.2 T) solvent diffusion plays a primary role in obtained DNP enhancements. Nevertheless, as molecular dynamic (MD) calculations show [10-12] in high magnetic fields other types of motions including a rotational diffusion with τ_{rot} could not be forgotten to explain high experimental results.

The coupling between two spin systems I and S may be expressed most generally in terms of equation

$$\langle I_z \rangle - \langle I_0 \rangle = \xi f [\langle S_z \rangle - \langle S_0 \rangle], \quad (2)$$

where $\langle I_z \rangle$ and $\langle S_z \rangle$ are the dynamic polarizations and $\langle I_0 \rangle$ and $\langle S_0 \rangle$ represent the thermal equilibrium condition; ξ is a coupling factor, f is a leakage factor which are examined in details below.

Coupling factor, ξ , with the maximal theoretical limits of -1 for scalar and $+0.5$ for dipole-dipole mechanisms, is a complicated function of many parameters and depends not only on the type of S - I interaction but through the spectral density function, J , it depends also on the field strength (ω_I and ω_S) and, through the correlation time, on the temperature and viscosity. Influence of the nitroxides' structure on coupling factor is up to now still under discussion even in well established low-field DNP experiments (see, for example, [13, 14] where nitroxides containing 5- and 6-membered rings are under consideration). Dipole-dipole mechanism is still dominant for the HF LS DNP by using nitroxides as polarizers leading to the negative DNP enhancement [1-3].

Leakage factor varying in the range [0..1] shows the fraction of the total relaxation rate due to nuclear-electron interaction and could be easily determined from NMR relaxation measurements:

$$f = 1 - \frac{T_1^{IS}}{T_1^I} \approx \frac{k_{\text{rel}} C T_1^I}{1 + k_{\text{rel}} C T_1^I}, \quad (3)$$

where T_1^I is a nuclear relaxation time (seconds in the case of water protons) in the absence of paramagnetic particles (pure solvent) and T_1^{IS} is that in the presence of the paramagnetics; k_{rel} is a relaxivity depending on the types of radical and solvent and on the experimental NMR frequency (magnetic field); C is a concentration of the paramagnetic particles.

It is believed [5, 15, 16] that coupling factor could be extracted from the measurements of k_{rel} with the external magnetic field, i.e. from the Nuclear Magnetic Resonance Dispersion (NMRD) profile. Nevertheless, the estimated in such a way values of the correlation times, τ , strongly depend on the model used and vary in the range (20-120) ps for the aqueous solutions of nitroxyl radicals at near room temperature [16, 17]. It leads us again to the need of re-examination of the existing models and experimental data obtained by different groups in different conditions.

The observable nuclear resonance enhancement, ε (DNP enhancement), is obtained by rearranging equation (2) as follows:

$$\varepsilon = \frac{\langle I_Z \rangle - \langle I_0 \rangle}{\langle I_0 \rangle} = \xi f \frac{[\langle S_Z \rangle - \langle S_0 \rangle]}{\langle S_0 \rangle} \frac{\langle S_0 \rangle}{\langle I_0 \rangle} = \xi f s \frac{\gamma_S}{\gamma_I}, \quad (4)$$

where γ_S and γ_I are the gyromagnetic ratios of electron and nuclear spins (γ_S is negative) and saturation factor, s , is introduced

$$s = \frac{[\langle S_0 \rangle - \langle S_Z \rangle]}{\langle S_0 \rangle}, \quad (5)$$

varying in the range 0 (no MW) to 1 (full saturation).

It is quite difficult to measure the value of s for the solutions of nitroxides at low MW power levels experimentally or even to calculate it. For the first approach, assuming the validity of the Bloch equations and homogenous line broadening of the non-interacting lines:

$$s = \frac{1}{n} \frac{\gamma_S^2 B_{\text{MW}}^2 T_{1e} T_{2e}}{(1 + \gamma_S^2 B_{\text{MW}}^2 T_{1e} T_{2e})} \quad (6)$$

where B_{MW} is a microwave field strength and n is a number of the lines, which should result in the maximal value of 1/3 for ^{14}N containing nitroxides assuming that the value of B_{MW} is less than the value of the nitroxide's hyperfine splitting.

Accepting the validity of Eq. (6), taken into account that the B_{MW}^2 is proportional to the MW power P_{MW} with the coefficient α (conversion factor) and inserting those into the Eq. (4), one can derive the linear dependence of the inverse DNP enhancement upon the inverse MW power, so called "power curve",

$$\frac{1}{\varepsilon_{\text{OE}}} = D \left(1 + \frac{E}{P_{\text{MW}}} \right) \equiv n \left(\frac{\gamma_S}{\gamma_I} f \xi \right)^{-1} \left(1 + \frac{1}{\gamma_S^2 T_{1e} T_{2e}} \frac{1}{\alpha P_{\text{MW}}} \right) \quad (7)$$

which can be experimentally measured. From the interception, D , of this curve one can extract the values of ξ , while the slope, E , is proportional to the $1/T_{1e} T_{2e}$. The Eq. (7) is still widely used for the estimations of ξ , T_{1e} and T_{2e} of different systems. The applicability of this approach for the liquid solutions of the nitroxides is one of the topics discussed in the present work.

3. Experimental part

Materials

Water soluble nitroxyl radical TEMPOL (4-hydroxy-2,2,6,6-tetramethyl-1-piperidiny-1-oxyl, CAS Number 2226-92-2, Fig. 1) was purchased from Sigma-Aldrich. The powder was diluted by distilled water bubbled by inert gas (Argon) for 15 min before to reduce the concentration of oxygen to obtain a stock solution with a concentration of about 5 M. The stock solution was diluted further in the same manner to get a series of samples with different concentrations. The concentrations were checked by X-band EPR measurements as well as in-situ measurements of relaxation times of the ^1H water protons T_{1l} and their paramagnetic shifts as explained in the text below.

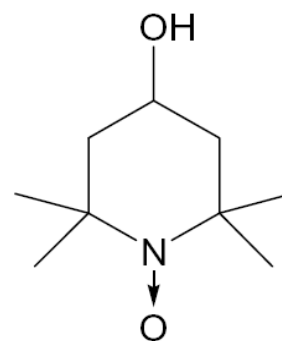


Figure 1. Organic nitroxide TEMPOL.

Methods

For NMR measurements a 400 MHz Bruker Avance NMR spectrometer was exploited. EPR measurements were done at 9 (X-band) and 95 GHz (W-band) using the continuous wave (cw) mode of Bruker Elexsys 580/680 spectrometer. Some experiments were done using the NMR/EPR/DNP abilities of Frankfurt LS DNP spectrometer operating at 260 GHz [18] and the cw-mode of the home-built 180 GHz (G-band) EPR spectrometer [19].

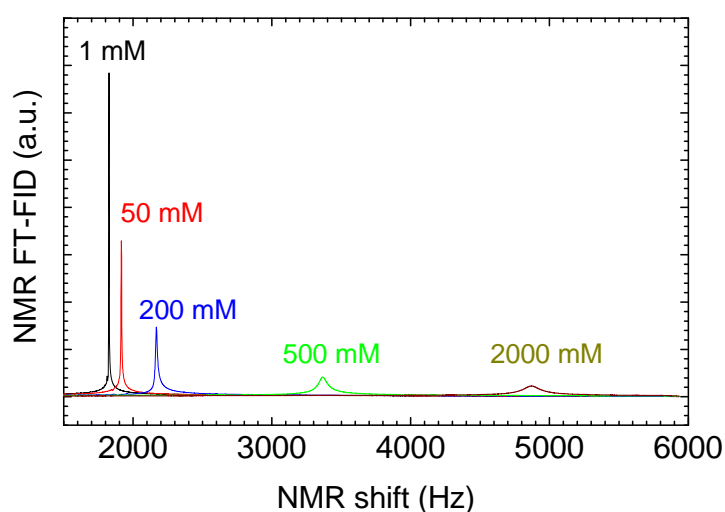


Figure 2. Dependence of the water proton Fourier transformed FIDs on TEMPOL concentration.

NMR measurements

The proton NMR longitudinal relaxation time T_{1l} obtained by applying inversion-recovery (IR) pulse sequence and relative peak position in “pure” water were measured to be about 3.4(1) s and 4.71(5) ppm at $T = 297$ K, correspondingly. These values and their changes with temperature measured in the temperature range (10-40) °C are in a good agreement with literature [20-22].

The influence of the paramagnetic TEMPOL on the linewidth of the Fourier transformed free induction decay signal (FT-FID) of water protons and on the corresponding NMR shift with concentration is demonstrated in Fig. 2. Based on the relaxation time measurements with TEMPOL concentration the leakage factor was measured (Fig. 3). This value does not depend on temperature in the investigated temperature range: both T_l and T_{1S} change with T in same manner (see Eq. 3). The value of $k_{\text{rel}} = 0.14(1) \text{ mM}^{-1}\text{s}^{-1}$ extracted using Eq. 3 is in a good agreement with literature data in such high fields [23].

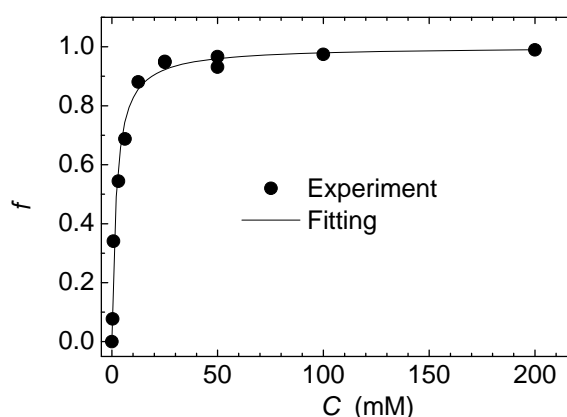


Figure 3. Concentration dependence of leakage factor (solid circles) and its fitting according to Eq. 3 with $k_{\text{rel}} = 0.14(1) \text{ mM}^{-1}\text{s}^{-1}$.

EPR measurements

The three line pattern observed in EPR experiments (well resolved at all available EPR frequencies for the concentrations of $C < 50$ mM) is due to the hyperfine interaction between the electronic spin with $S = 1/2$ and one nuclear spin with $I = 1$ as a case for ^{14}N . The components of g -factors and hyperfine constant A measured at different frequencies in liquid and in frozen state are given in Table 1 and correspond to the known from the literature [24, 25].

With the known components of g and A tensors, the isotropic rotational correlation time τ_c can be extracted from EPR spectra. This was done by the simulating the experimental data using the built-in tools of the EasySpin package for Matlab [26] as well as by using the self-written program based on the model described in [27] which give identical value of about 18(2) ps at $T = 295(2)$ K. (Uncertainty is ascribed mainly to the difference in temperature conditions in different EPR spectrometers).

Investigations of the temperature dependence of τ_c at different frequencies show that at least in the temperature range (279-313) K it shortens according to the ratio of water viscosity over T (η/T) tabulated for water in [28].

Sufficiently rapid rotation of the molecules of the mono-radicals in low viscosity liquids leads to complete averaging of the dipole-dipole interaction. Thus, in the EPR and DNP spectra of solutions with a sufficiently low viscosity it is possible to detect only the isotropic exchange interaction (Heisenberg exchange, characterized by the exchange rate denoted as τ_H or exchange constant k_{ex}). The value of the exchange constant could be extracted from the EPR lines' shift and broadening with concentration. In this work it is done from the broadening of the central line according to [29, 30]. The values extracted in such a way are the same for different magnetic fields (EPR frequencies) in correspondence with literature [31] and are about $k_{ex} = 1.8(1) \cdot 10^9 \text{ M}^{-1}\text{s}^{-1}$ at $T = 293(2)$ K (Fig. 4).

It could be expected that due to the very fast Heisenberg exchange at very high concentrations after the "coalescence" of all three lines into the single one the resulting line will tend further to narrow. The EPR results show, however, that at $C > 500$ mM the EPR line does not change much and becomes even slightly broader (Fig. 5) at all MW frequencies available. This fact can be explained by the

Table 1. Literature and experimental data of components of hyperfine and g -tensors and exchange interaction rates (normalized to the temperature and viscosity) of the nitroxide TEMPOL in water.

Parameter	Literature Data [24, 25]	Experiment
g_{xx}	2.0085(2)	2.0086(3)
g_{yy}	2.0061(1)	2.0060(2)
g_{zz}	2.0021(3)	2.0020(4)
g_{iso}	2.0056(2)	2.0055(3)
A_{xx} [G]	6(1)	6(1)
A_{yy} [G]	6(1)	6(1)
A_{zz} [G]	36.4(1)	36.4(1)
A_{iso} [G]	16.5(4)	16.6(3)
$K_{exch} \cdot \eta/T$ [cP/M ⁻¹ s ⁻¹]	$6.2 \cdot 10^6$	$6.4(3) \cdot 10^6$

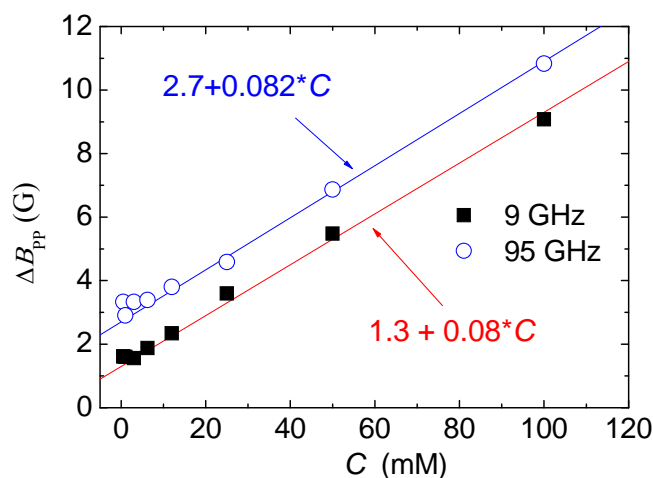


Figure 4. Concentration dependencies of the linewidths of the central line of ^{14}N three line nitroxide pattern taken at $T = 293$ K at two different frequencies to demonstrate the difference in the absolute values but practically identical slope.

influence of the dipole-dipole interaction between the electronic spins at such high concentrations.

The EPR linewidth and k_{ex} strongly depend on the temperature. For example, for $C = 500$ mM the linewidth of the single EPR line at $T = 279$ K G-band (magnetic field of 6.4 T) is $\Delta B_{\text{pp}} = 15.8$ G while at $T = 310$ K it narrows to $\Delta B_{\text{pp}} = 9.9$ G. The temperature changes in W-band range (95 GHz) were measured by E. Kryukov et al. in a wide temperature range [32]. Our results obtained in X- and G-bands agree with those and confirm the dependence $d\Delta H/dC = E(T/\eta)$ [33] with $E = 3.15(20) \cdot 10^{-3}$ (P·G)/(M·K) using the data of (η/T) from [28].

4. Discussion

Low values of k_{rel} obtained in the field of 9.4 T for the aqueous solutions of the nitroxide TEMPOL inevitably result in demand to use high nitroxide concentrations to achieve perceptible DNP enhancement through the proper leakage factor (cf. Fig. 3, Eqs. 3, 4). The value $f = 0.84$ is achieved in the field of 9.4 T at $C \approx 20$ mM. Therefore, while the optimal concentrations reported for the low-field (earth field) experiments is about (1-2) mM [34, 35] in high-field experiments of (3.4-10) T the concentrations in the range (6-40) mM are exploited [11, 15, 16, 23, 32, 36, 37]. Even higher concentrations would be used for the higher fields corresponding to the (600-1000) MHz proton NMR frequencies. From this point of view (high leakage factor) TEMPOL with its excellent solubility in H_2O is a good polarizing agent.

Nuclear relaxation time T_1^{IS} shortens drastically with concentration that can through the shorter repetition times significantly reduce the duration of NMR/MRI experiments. As the experimental data show [4, 15, 23, 37], build-up curve of the nuclear polarization growth caused by the *in-situ* OE DNP effect in liquid solutions of nitroxides is characterized by practically identical with T_1^{IS} time. Short repetition time (seconds and less) of the *in-situ* OE DNP experiments especially at high concentrations can be regarded as a tremendous advantage over others exploiting alternating experimental schemes and DNP mechanisms. But such problems as toxicity and bio-compatibility should be taken into the consideration for some of applications.

The paramagnetic shift should not be forgotten in DNP experiments to detect an NMR line at the right position and to extract the NMR parameters influenced by the MW irradiation properly [38]. As it is shown above, the shift along with the T_1^{IS} measurements could be used for the control of the TEMPOL concentration and for the sample temperature monitoring in high-resolution NMR experiments though the temperature itself does not influence the leakage factor much.

Let us now consider different factors influencing the saturation. According to the simple model (Eq. 6) to achieve the maximum saturation high MW power should be applied to the paramagnetic solution with the long electronic relaxation times. Due to the different mechanisms of the inhomogeneous broadening (anisotropy of g and A tensors, homogeneity and stability of the external magnetic fields, etc) the EPR linewidth become broader with B_0 (i.e. T_{2e} becomes shorter, cf. Fig. 4) and, therefore, it is much more difficult to achieve a full saturation in high fields.

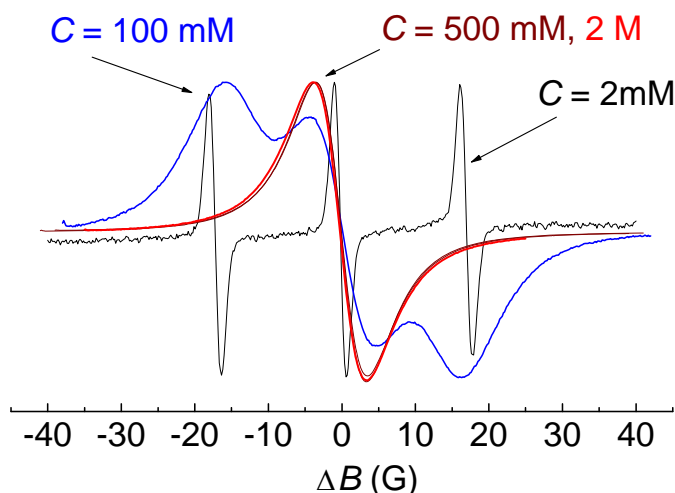


Figure 5. Concentration dependence of the normalized EPR spectra taken in X-band at $T = 298$ K. $\Delta B = B - B_{0C}$ where B_{0C} is the resonance position of the central hyperfine component of the EPR spectra.

Up to now there are no direct measurements of electronic relaxation times in aqueous solutions of nitroxides in high fields. The recent experiments show that T_{1e} is dropping with MW frequency at $\nu_s > 40$ GHz [39]. Estimations in the range of (100-1000) ns are given in literature [18, 27, 40]. As can be concluded from the low-field experiments ($\nu_s < 40$ GHz), deuteration of the nitroxyl, deuteration of solvent, or replacement of natural-abundance nitrogen by nitrogen-15 in the nitroxyls cause less than 10% change in T_{1e} [41]. Surprisingly, the values of T_{1e} seem to be independent on the concentration of the nitroxides up to the values of $C = 200$ mM at least as measured at $\nu_s = 9$ GHz by Longitudinally Detected EPR [42, 43] while the dissolved in water paramagnetic oxygen can drastically shorten T_{1e} up to factor 3 as measured in low field experiments [43] shrinking, therefore, through the saturation factor the obtainable OE DNP enhancement.

Based on the experimental and theoretical results presented in [27], the DNP profile (dependence of the DNP enhancement on the small changes in B_0 or on the value of the MW frequency) through the saturation factor follows exact the EPR profile (integrated EPR spectra). It defines the difference in the right choice of the position of the MW pumping to achieve the better saturation with frequency and concentration. At low concentration in high fields (6-10 T) the first hyperfine line (position of which is concentration dependant) is preferable while in low fields (0.3-1 T) the central one. At higher concentrations the central one is the best option for all the frequencies. In addition, the position of the central line is defined by the isotropic value of g -tensor, i.e. do not change with concentration.

To avoid the water overheating caused by MW power, different resonance structures are usually exploited in OE DNP experiments geometry of which allow to amplify the value of B_{MW} and to reduce the electrical component of the electromagnetic field. Using the values of B_{MW} in the range (0.8-1) G known from the helical resonance structure of the of Frankfurt LS DNP spectrometer operating at low MW power of less than 45 mW [11, 18] the saturation factor in the framework of the model developed in [27] (in which the rigorous treatment of the nitroxide saturation based on Redfield theory and using modified Bloch Equations in presence of exchange interaction and taken into account the nitrogen relaxation is performed) was calculated. The next input parameters are mandatory for this:

- the values of g -and A -tensors (Table 1);
- characteristic correlation time of the rotational motion, τ_C ;
- rate of the Heisenberg exchange, τ_H which is a function of concentration and temperature;
- MW field strength, B_{MW} ;
- value of the external magnetic field, B_0 ;
- value of T_{1e} ;
- additional inhomogeneous contribution into the linewidth of the nitroxide EPR spectra at high fields.

The simulations are presented in Fig. 6 and 7.

Fig. 6 illustrates the dependence of the saturation factor on the position of the MW pumping for different spin-lattice electronic relaxation times (because T_{1e} is an unknown value). The relation between the best position for the MW pumping to get the highest OE DNP enhancement and T_{1e} has something in common with the concentration topic discussed above: for the longer relaxing centers the central line is preferable with variations for the fast-relaxing centres depending on the value of B_0 . As it can be seen even at low MW power (B_{MW} is less than the EPR linewidth of each of the hyperfine components even at very low concentrations) saturation factor of more than 1/3 in contradiction with Eq. 6 could be achieved. Applying more MW power the values up to $s = 0.9$ are approached in the fields of 3.4 T [44]. It means that the simple model of the calculation of saturation factors (Eq. 6) and extraction of DNP and EPR parameters from the power curve by using Eq. 7 are not applicable in the case of liquid solutions of the nitroxides. Nevertheless, in the case of the single merged line (high concentrations) they may be used with a certain accuracy.

The presence of the Heisenberg exchange interaction makes complicated not only the concentration dependence of the EPR spectra but also the saturation curve and, consequently, the obtained DNP enhancement as Fig. 7 demonstrates. For some chosen experimental parameters at $B_0 = 9.4$ T the concentration curve fs reveal clearly the plateau at $C = (10-20)$ mM (we suppose implicitly that ξ in Eq. 4 is concentration independent). Then it is only slightly goes down (due to the fact that f is growing while saturation due to the EPR line broadening caused by the exchange interaction is decreasing). It worth noting that the obtained local maxima in concentrations for s and ε could have different values as it is a case for the chosen parameter set. The value of the local maximum (product fs) depends also on the other parameters. As preliminary calculations show, the higher are the values of B_{MW} and B_0 the more the position of the local maximum is shifted to the higher concentrations. At $C > 100$ mM the EPR spectrum starts to merge into the single line facilitating in this manner a saturation. Consequently, the product fs is growing with C while f does not change and is close to its maximal value. According to the EPR spectra, the growth with concentration should continue up to the $C \approx 500$ mM. No experimental data of OE DNP for such high concentrations are known to author. To quantify this effect at higher concentrations a role and a quantitative ratio of the electron-electron dipole-dipole interaction should be clarified and calculated which is still not done in the nitroxide research to the best of the author knowledge.

During the process of the preparation of this work for publication a paper that confirms experimentally high DNP enhancements for high concentrations of nitroxides has appeared [45]. The authors have measured OE DNP at $B_0 = 9.24$ T on the water protons in the water-TEMPOL system with the nitroxide's concentration of $C = 1$ M. The DNP enhancements $\varepsilon = -14$ at room temperature and -80 at 160°C (overheated water solution) were achieved. The saturation factor $s = 1$ at $P_{MW} \approx 200$ mW was reached.

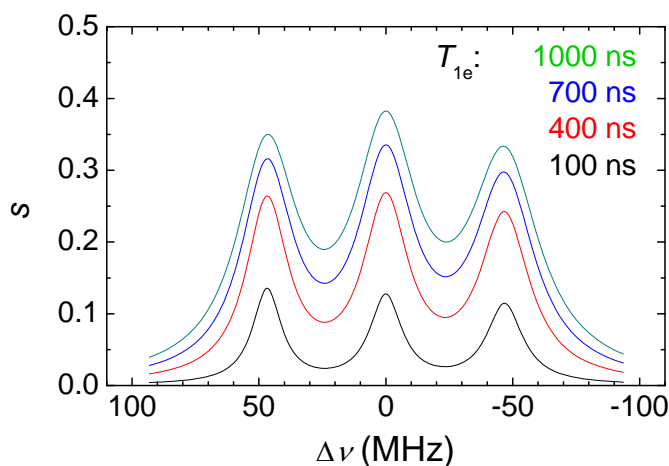


Figure 6. Saturation profiles for the saturation factor of the aqueous solution of TEMPOL calculated for $C = 10$ mM, $B_0 = 9.4$ T, $B_{MW} = 0.84$ G and for $T_{1e} = 100, 400, 700$ and 1000 ns (from the lower to the upper curves), consequently. $\Delta\nu = \nu_s - \nu_{s0}$; the EPR frequency resonant to the central hyperfine line is denoted as ν_{s0} .

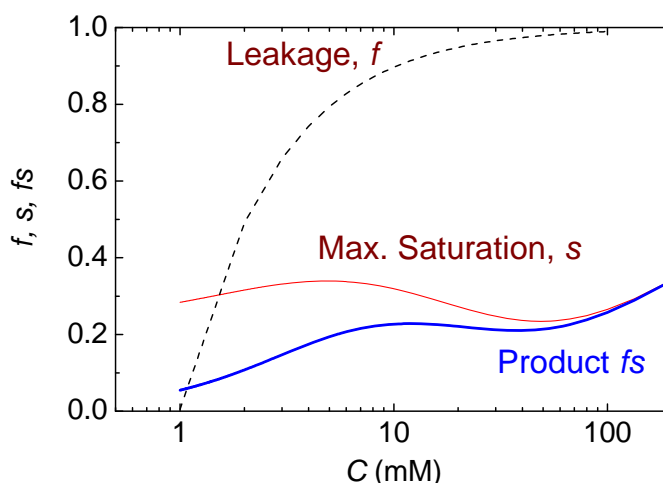


Figure 7. Experimentally measured leakage factor, calculated maximal saturation factor for $B_{MW} = 0.84$ G and $T_{1e} = 700$ ns in the magnetic field of $B_0 = 9.4$ T and their product, fs as the functions of TEMPOL concentration presented in a semi-logarithmic scale.

The most problematic is a task to follow the temperature dependence of s . Temperature behavior of many parameters can be extracted from the experiment (see Section 3) but not that of T_{1e} . Intuitively, T_{1e} should drop with T lowering the value of s (cf. Fig. 6). Simultaneously, the Heisenberg exchange rate decreases and rotational correlation time shortens that generally should elevate s . In [37] it was supposed that these oppositely directed mechanisms compensate each other at least in the investigated temperature range and the temperature curve of OE DNP enhancement is mainly defined by the temperature behavior of the TEMPOL-water coupling factor (Eq. 4).

As it was pointed out it is quite tricky to extract the coupling factor for the aqueous solutions of nitroxides experimentally. At present moment it is thought that the MD calculations performed by D. Sezer for TEMPOL in water [10] for the magnetic field strength from 0.33 up to 12 T for three temperature values: 25, 35 and 45 °C are the most reliable. As expected, the coupling factors decrease substantially upon increase in the magnetic field: from 30 % at $B_0 = 0.33$ T down to 1.3 % at $B_0 = 12$ T. Temperature raise from 25 °C to 45 °C significantly influences ξ in high magnetic fields (up to 2 times for $B_0 = 12$ T) but only slightly at $B_0 = 0.33$ T (on just 13 %). Rapid, nearly linear temperature raise of ξ in high magnetic fields in the temperature range up to 60 °C is experimentally confirmed for 3.4 T [32] and 9.2 T [37]. The question whether the classical translational model only (see Eq. 1) could adequately describe the OE DNP results in high magnetic fields is still hotly debated [10, 32, 37, 46]. The data obtained in this work show that the temperature dependence of both rotational and translational correlation times follow η/T curve and, therefore, from the experimental point of view their personal contributions are not distinguishable in the cumulative temperature curve. Study of the nitroxides' systems with very similar structure but different τ_c would help to separate these contributions.

5. Conclusion and perspectives

DNP measurements [1-3, 23, 32, 45], NMR and multifrequency EPR characterization for the aqueous solutions of the nitroxide TEMPOL in the temperature range (10-40) °C show that this system could give a perceptible OE DNP enhancement in low and high (> 12 T) magnetic fields even by using low microwave power sources to polarize the electron spin system. Strong linear temperature dependence of OE DNP enhancement is expected for this system in high fields. Optimal concentration to obtain the maximal OE DNP enhancement is defined by the interplay of leakage and saturation factors and could be estimated from the NMR and EPR data. Based on the estimations of saturation factor it could be expected that the values of optimal concentration for higher (12 T, corresponding to 600 MHz proton frequency) magnetic fields would be either in the range 40-80 mM depending on the technical characteristics of the DNP spectrometers (MW power, conversion factor of the resonance structure, etc) or > 500 mM. Excellent water solubility of TEMPOL could facilitate its usage for the high-field OE DNP application.

The systematic study of various nitroxide systems and solvents in several magnetic fields are planned to separate different contributions into the OE DNP mechanism and to investigate the possibilities of using nitroxides for DNP study of the water/oil binary mixtures.

Acknowledgments

The work was supported by the Ministry of Science and Education of the Russian Federation (Project number 02.G25.31.0029). The author is indebted to Thomas Prisner, Mark Prandolini, Vasyil Denysenkov, Deniz Sezer, Burkhard Endeward, George Mamin, Sergei Orlinkii, Murat Tagirov, Sergei Nikitin and Vladimir Skirda for the multidimensional experimental and theoretical assistance, brilliant ideas and inspiration.

References

1. Prisner T.F., Koeckenberger W. (Ed.) Dynamic Nuclear Polarization: New Experimental and Methodology Approaches and Applications in Physics, Chemistry, Biology and Medicine, *Appl. Magn. Reson.* **34**, 213-544 (2008)
2. Griffin R.G., Prisner T.F. (Ed.) High field dynamic nuclear polarization - the renaissance, *Phys. Chem. Chem. Phys.* **12**, 5725-5928 (2010)
3. Atsarkin V.A., Koeckenberger W. (Ed.) The Different Magnetic Resonance Communities Join Forces for Progress in DNP, *Appl. Magn. Reson.* **43**, 1-310 (2012)
4. Potenza J. *Adv. Mol. Relax. Proc.* **4**, 229 (1972)
5. Hausser K.H., Stehlik D. *Adv. Magn. Reson.* **3**, 79 (1968)
6. Dweck R.A., Richards R.E., Taylor D. *Ann. Rev. NMR. Spectrosc.* **2**, 293 (1969)
7. Overhauser A.W. *Phys. Rev.* **92**, 411 (1953)
8. Abragam A. *The Principles of Nuclear Magnetism*, Clarendon Press, Oxford (1961)
9. Gafurov M, Lyubenova S, Denysenkov V, Ouari O, Karoui H, Le Moigne F, Tordo P, Prisner T. *Appl. Magn. Reson.* **37**, 505 (2009)
10. Sezer D, Prandolini M.J., Prisner T.F. *Phys. Chem. Chem. Phys.* **11**(31), 6626 (2009)
11. Denysenkov V.P., Prandolini M.J., Gafurov M., Sezer D, Endeward B., Prisner T.F. *Phys. Chem. Chem. Phys.* **12**, 5786 (2010)
12. Sezer D. *Phys. Chem. Chem. Phys.* **15**, 526 (2013)
13. Grucker D., Guiberteau T., Eclancher B, Chambron J, Chiarelli R, Rassat A, Subra G, Gallez B. *Journ. Magn. Reson. B* **106**, 101 (1995)
14. Armstrong B.D., Soto P, Shea E., Han S. *Journ. Magn. Reson.* **20**, 137 (2009)
15. Bennati M., Luchinat C., Parigi G., Türke M.-T. *Phys. Chem. Chem. Phys.* **12**, 5902 (2010)
16. Höfer P., Parigi G, Luchinat C, Carl P, Guthausen G, Reese M, Carlomagno T, Griesinger Ch., Bennati M. *J. Am. Chem. Soc.* **130**, 3254 (2008)
17. Goldammer E.V., Kreysch W., Wenzel H. *Journ. Solution Chem.* **7**, 197 (1978)
18. Denysenkov V.P., Prandolini M.J., Krahn A, Gafurov M., Endeward B., Prisner T.F. *Appl. Magn. Reson.* **34**, 289 (2008)
19. Hertel M.M., Denysenkov V.P., Bennati M., Prisner T.F. *Magn. Res. Chem* **43**, S248 (2005)
20. Simpson J.H., Carr H.Y. *Phys. Rev.* **111**, 1201 (1958)
21. Teng Q. *Structural Biology: Practical NMR Applications*, Springer, New-York (2005), p. 19
22. Wu T., Kendell K.R., Felmlee J.P., Lewis B.D., Ehman R.L. *Med. Phys.* **27**, 221 (2000)
23. Prandolini M.J., Denysenkov V., Gafurov M., Lyubenova S., Endeward B., Bennati M., Prisner T. *Appl. Magn. Reson.* **34**, 399 (2008)
24. Buchachenko A.L., Wasserman A.M. *Stable Radicals. Electronic Structure, Reactivity and Application*, Khimiya, Moscow (1973) (in Russian)
25. Kovarskii A.L., Wasserman A.M, Buchachenko A.L. *Journ. Magn. Reson.* **7**, 225 (1972)
26. Stoll S., Schweiger A. *Journ. Magn. Reson.* **178**, 42 (2006)
27. Sezer D, Gafurov M, Prandolini M.J., Denysenkov V.P., Prisner T.F. *Phys. Chem. Chem. Phys.* **11**, 6638 (2009)
28. Cho C.H., Urquidi J., Singh S., Wilse Robinson G. *J. Phys. Chem. B* **103**, 1991 (1999)
29. Sueishi Y., Nishimura N., Hirata K., Kuwata K. *Bull Chem. Soc. Jpn.* **61**, 4253 (1988)
30. Ablett S., Barratt M.D., Franks F.S. *Journ. Solution Chem.* **4**, 797 (1975)

31. Chemerisov S.D., Kokorin A.I., Grinberg O.Ya., Lebedev Ya.S. *Appl. Magn. Reson.* **9**, 37 (1995)
32. Kryukov E.V., Pike K.J., Tam T.K.Y., Newton M.E., Smith M.E., Dupree R. *Phys. Chem. Chem. Phys.* **13**, 4372 (2011)
33. Berner B., Kivelson D. *Journ. Phys. Chem.* **83**, 1406 (1979)
34. Yamada K.-I., Kinoshita Y., Yamasaki T., Sadasue H., Mito F., Nagai M., Matsumoto S., Aso M., Suemune H., Sakai K., Utsumi H. *Arch. Pharm. Chem. Life Sci.* **341**, 548 (2008)
35. Utsumi H., Yamada K.-I., Ichikawa K., Sakai K., Kinoshita Y., Matsumoto S., Nagai M. *PNAS* **103**, 1463 (2006)
36. Prandolini M.J., Denysenkov V.P., Gafurov M., Endeward B., Prisner T.F. *J. Am. Chem. Soc.* **131**, 6090 (2009)
37. Gafurov M., Denysenkov V., Prandolini M.J., Prisner T. *Appl Magn Reson.* **43**, 119 (2012)
38. Alekseev B.F., Sobotkovskii B.E. *Radiophysics and Quantum Electronics* **12**, 189 (1969) (*Izvestiya VUZ. Radiofizika* **12**, 236 (1969), in Russian)
39. Froncisz W., Camenisch T.G., Ratke J.J., Anderson J.R., Subczynski W.K., Strangeway R.A., Sidabras J.W., Hyde J.S. *J. Magn. Reson.* **193**, 297 (2008)
40. Hofbauer W., Earle K.A., Dunnam C.R., Mościcki J.K., Freed J.H. *Rev. Sci. Instrum.* **75**, 1194 (2004)
41. Du J.-L., Eaton G.R., Eaton, S.S. *Journ. Magn. Reson. A.* **115**, 213 (1995)
42. Atsarkin V.A., Demidov V.V., Vasneva G.A., Odintsov B.M., Belford R.L., Raduchel B., Clarkson R.B. *Journ. Phys. Chem. A* **105**, 9323 (2001)
43. Panagiotelis I., Nicholson I, Hutchison J.M.S. *Journ. Magn. Reson.* **149**, 74 (2001)
44. Türke M-T, Bennati M. *Phys. Chem. Chem. Phys.* **13**, 3630 (2011)
45. Neugebauer P., Krummenacker J.G., Denysenkov V.P., Parigi G, Luchinat C., Prisner T.F. *Phys. Chem. Chem. Phys.* **15**, 6049 (2013)
46. Villanueva-Garibay J.A., Annino G., van Bentum P.J.M., Kentgens A.P.M. *Phys. Chem. Chem. Phys.* **12**, 5846 (2010)